Interactions between Electron and Proton Currents in Excised Patches from Human Eosinophils

Gábor L. Petheö,[1] Andrés Maturana,[1] András Spät,[2] and Nicolas Demaurex[1]

[1]Department of Physiology, University of Geneva Medical Center, CH-1211 Geneva 4, Switzerland
[2]Department of Physiology and Laboratory of Cellular and Molecular Physiology, Semmelweis University and Hungarian Academy of Sciences, H-1444 Budapest, Hungary

ABSTRACT The NADPH–oxidase is a plasma membrane enzyme complex that enables phagocytes to generate superoxide in order to kill invading pathogens, a critical step in the host defense against infections. The oxidase transfers electrons from cytosolic NADPH to extracellular oxygen, a process that requires concomitant H^+ extrusion through depolarization-activated H^+ channels. Whether H^+ fluxes are mediated by the oxidase itself is controversial, but there is a general agreement that the oxidase and H^+ channel are intimately connected. Oxidase activation evokes profound changes in whole-cell H^+ current (I_H), causing an approximately −40-mV shift in the activation threshold that leads to the appearance of inward I_H. To further explore the relationship between the oxidase and proton channel, we performed voltage-clamp experiments on inside-out patches from both resting and phorbol-12-myristate-13-acetate (PMA)-activated human eosinophils. Proton currents from resting cells displayed slow voltage-dependent activation, long-term stability, and were blocked by micromolar internal [Zn^{2+}]. I_H from PMA-treated cells activated faster and at lower voltages, enabling sustained H^+ influx, but ran down within minutes, regaining the current properties of nonactivated cells. Bath application of NADPH to patches excised from PMA-treated cells evoked electron currents (I_e), which also ran down within minutes and were blocked by diphenylene iodonium (DPI). Run-down of both I_H and I_e was delayed, and sometimes prevented, by cytosolic ATP and GTP-γ-S. A good correlation was observed between the amplitude of I_e and both inward and outward I_H when a stable driving force for e^- was imposed. Combined application of NADPH and DPI reduced the inward I_H amplitude, even in the absence of concomitant oxidase activity. The strict correlation between I_e and I_H amplitudes and the sensitivity of I_H to oxidase-specific agents suggest that the proton channel is either part of the oxidase complex or linked by a membrane-limited mediator.

KEY WORDS: physiology • NADPH–oxidase • zinc • phagocyte • patch-clamp

INTRODUCTION

Phagocytic white blood cells such as neutrophils or eosinophils are key effectors of our innate immune system, and are the first line of defense against bacterial, fungal, and parasitic infections. The main weapon of these phagocytic cells is the NADPH–oxidase, a multisubunit enzyme complex that transports electrons from cytoplasmic NADPH to molecular oxygen, thereby generating high amounts of superoxide free radicals ($O_2^{\cdot -}$). The relatively harmless superoxide anion is then converted into more reactive oxygen species that are able to kill invading pathogens. As these reactive oxygen species are also toxic to the host cells, the activation and inactivation of the oxidase is a finely regulated process that takes places only at the right time and place (for reviews on the oxidase function see Geiszt et al., 2001; Babior et al., 2002; Bokoch and Diebold, 2002; Vignais, 2002).

The fully activated oxidase complex contains at least two membrane-bound proteins, $gp91^{phox}$ and $p22^{phox}$, that form the flavocytochrome b_{558} heterodimer (Wallach and Segal, 1996; phox for phagocyte oxidase). The highly glycosylated $gp91^{phox}$ is a transmembrane protein that comprises putative binding sites for NADPH and flavin cofactors at its COOH terminus (Babior et al., 2002), as well as two heme groups embedded in the plasma membrane and coordinated noncovalently by four histidine residues within $gp91^{phox}$ third and fifth transmembrane domains (Biberstine-Kinkade et al., 2001). While $gp91^{phox}$ is the core electron transporting enzyme of the oxidase, $p22^{phox}$ seems to have mainly adaptor function and appears to be required for proper maturation and membrane targeting of the $gp91^{phox}$ subunit (DeLeo et al., 2000).

The online version of this paper contains supplemental material.

Address correspondence to Dr. Nicolas Demaurex, Department of Physiology, University of Geneva Medical Center, 1 Michel-Servet, CH-1211 Geneva 4, Switzerland. Fax: (41) 22-379-5402; email: Nicolas.Demaurex@medecine.unige.ch

Abbreviations used in this paper: CGD, chronic granulomatous disease; DPI, diphenylene iodonium chloride; NADPH, nicotinamide adenine dinucleotide phosphate; NBT, p-nitro-blue tetrazolium chloride; phox, phagocyte oxidase.

J. Gen. Physiol. © The Rockefeller University Press • 0022-1295/2003/12/713/14 $8.00
Volume 122 December 2003 713–726
http://www.jgp.org/cgi/doi/10.1085/jgp.200308891

The activation of the oxidase also requires membrane translocation of four cytosolic proteins: a heterotrimer composed of $p67^{phox}$, $p47^{phox}$, and $p40^{phox}$ (Lapouge et al., 2002), and a small guanosine triphosphatase (GTPase) protein, either Rac1 or Rac2 (Bokoch and Diebold, 2002). Translocation of the heterotrimer requires the phosphorylation of $p47^{phox}$ and the presence of Rac in its GTP-bound form (for reviews on the oxidase assembly and structure see Babior et al., 2002; Bokoch and Diebold, 2002; Vignais, 2002). Optimal assembly and activation of the oxidase complex is further promoted by arachidonic acid (Doussiere et al., 1996; Shiose and Sumimoto, 2000; Foubert et al., 2002) and by products of phosphatidylinositol 3-kinase (Kanai et al., 2001; Karathanassis et al., 2002; Brown et al., 2003; Stahelin et al., 2003). The importance of a functional oxidase is underscored by the chronic granulomatous disease (CGD), a disease associated with mutations within one of the phox proteins, predominantly the core $gp91^{phox}$ subunit. CGD patients have impaired phagocytic NADPH–oxidase activity and suffer from severe and recurrent infections (for reviews on CGD see Goldblatt and Thrasher, 2000; Geiszt et al., 2001).

Sustained activation of the oxidase involves the constant flow of electrons across the plasma membrane, a process that is electrogenic and requires the movement of a compensating charge (Henderson et al., 1987; Schrenzel et al., 1998). Furthermore, as superoxide anions are being generated by the oxidase, H^+ ions are left behind in the cytoplasm as a result of the conversion of $NADPH + H^+$ into $NADP^+ + 2H^+$. If uncompensated, the sustained transfer of electrons across the membrane would lead to extreme depolarization and cytoplasmic acidification, conditions that would strongly interfere with the oxidase activity. To account for both charge and pH compensation, the core component of the oxidase, $gp91^{phox}$, has been proposed very early on to contain a pathway for H^+ ions (Henderson et al., 1995), like mitochondrial cytochromes. Proton efflux could be demonstrated in phagocytes by pH measurements (Kapus et al., 1992), and was shown to be closely linked with the activation, but not with the redox function, of the oxidase (Nanda et al., 1994). Direct evidence for voltage-gated proton channels was subsequently provided by patch-clamp recordings in phagocytic cell lines, neutrophils, and eosinophils (DeCoursey and Cherny, 1993; Demaurex et al., 1993; Gordienko et al., 1996; Schrenzel et al., 1996). Voltage-gated proton channels conduct H^+ ions very efficiently down their electrochemical gradient, thereby shunting the voltage and pH gradient across the membrane and are required for sustained activation of the oxidase (Henderson et al., 1988; DeCoursey et al., 2003).

Proton channels are activated by depolarization and cytosolic acidification, ensuring a functional coupling to the oxidase. The regulation of the oxidase and of the proton-channel overlap in many respects, as both phagocytic H^+ channels and oxidase can be activated by arachidonic acid (Cherny et al., 2001), PMA (DeCoursey et al., 2001), and by intracellular application of a mixture of ATP, GTP-γ-S, and Ca^{2+} (Schrenzel et al., 1998; Banfi et al., 1999). In whole-cell recordings from human eosinophils, oxidase activation by GTP-γ-S was associated with H^+ currents that activated at lower voltages, and had faster activation kinetics and slower inactivation kinetics, an effect that was not observed in cells from CGD patients lacking the $gp91^{phox}$ or $p47^{phox}$ protein (Banfi et al., 1999). This interconnection between phagocytic proton channels and oxidase led us (Banfi et al., 1999) and others (Henderson and Meech, 1999) to postulate that the H^+ pathway is either contained within, or is closely associated with the membrane components of the oxidase. Consistent with the channel nature of $gp91^{phox}$, heterologous expression of $gp91^{phox}$ and of its recently cloned homologues NOX1 and NOX5 produced voltage-activated proton currents in CHO and HEK-293 cells (Henderson and Meech, 1999; Banfi et al., 2000, 2001). However, these cell lines display endogenous H^+ currents, raising the possibility that $gp91^{phox}$ and its homologues might function as channel modulators, rather than forming a channel themselves. Consistent with this hypothesis, reconstitution of a fully functional oxidase in COS-7 cells, which lack endogenous H^+ currents, was not associated with measurable proton currents (Morgan et al., 2002). Because of these conflicting results, it is not clear yet whether $gp91^{phox}$ is a proton channel or a channel modulator, as discussed in detail in a recent series of perspective articles (DeCoursey et al., 2002; Henderson and Meech, 2002; Maturana et al., 2002; Touret and Grinstein, 2002).

The modulation of proton currents in cells with an active oxidase as well as their up-regulation during $gp91^{phox}$ heterologous expression indicate that, if $gp91^{phox}$ is not a channel, it is closely associated with the channel protein(s). However, purification of cytochrome b_{558} aggregates from resting phagocytes (Nugent et al., 1989) or copurification of the cytochrome with membrane-bound Rap1 GTPase from activated phagocytes (Quinn et al., 1989) failed to detect any additional membrane protein other than $gp91^{phox}$ and $p22^{phox}$. Furthermore, given the importance of proton channels for charge and pH compensation during the respiratory burst, mutations that alter the channel function are expected to strongly affect superoxide production and to cause a CGD phenotype. However, so far no CGD case could be attributed to a protein distinct from the NADPH–oxidase complex. Instead, most mutations leading to the CGD phenotype map to the $gp91^{phox}$ core component of the oxidase (Goldblatt

and Thrasher, 2000; Vignais, 2002). Conversely, all of the known mutations that suppress H^+ currents or alter its properties are located within the oxidase complex, preferentially in gp91^{phox} (Banfi et al., 1999; Henderson and Meech., 1999; Maturana et al., 2001). Therefore, at this stage, the simplest and most economical theory is still, in our view, the original postulate that the proton pathway is located within the oxidase complex.

The interaction between proton channels and the NADPH–oxidase has so far not been studied under conditions that allows a stringent control of the microenvironment near the plasma membrane. This renders the interpretation difficult, because activation of the oxidase and of its associated channel generates local changes in pH, NADPH, and $O_2^{\cdot -}$ which, in turn, modulate the activity of the transport proteins being studied. In this study, we describe measurement of the phagocytic NADPH–oxidase-generated electron (e^-) current and proton (H^+) current in inside-out patches from human eosinophils. To our knowledge, this is the first report that investigates these two functions in a cell-free system. The results obtained with this approach further strengthen the hypothesis that, in human eosinophils, the proton channel and the NADPH–oxidase interact either physically or via a membrane-limited mediator.

MATERIALS AND METHODS

Patch-clamp Measurements

Voltage-clamp patch-clamp experiments were performed on inside-out membrane patches excised from human eosinophils. Preparation of human eosinophils was performed as previously described (Schrenzel et al., 1996) except for minor modifications as follow. Cells were prepared from venous blood drawn from nonatopic healthy adult males after obtaining their informed consent. Cells were kept on 4°C in closed, airtight, polypropylene Eppendorf tube (Treff AG) at ~500 cell/μl density in culture media (composition given below). In preliminary tests eosinophils stored this way were able to respond to PMA and produced electron current in inside-out patches even after 72 h of storage. Cells stored for more than 60 h were not used for the experiments presented in this paper.

For patch-clamp experiments cells were placed on glass coverslip in the bottom of a conical recording chamber. Cells and pipette electrode were visualized using an inverted microscope (Axiowert 10; ZEISS). In sterile filtered solutions high quality seals (>50 GΩ) formed spontaneously after gently attaching the pipette tip to the cell surface followed by a slight, transient suction through the pipette electrode. Stronger and sustained suction was rarely required and resulted in larger patches. Patch excision was achieved by fast, vertical retraction of the pipette tip from the cell surface. In some cases (mainly when strong suction had to be applied and with smaller tip openings) instead of inside-out patch an excised vesicle was formed this way and the pipette tip had to be lifted very briefly (<1 s) into air to establish the right configuration. This intervention, however, often interfered with long-term seal stability. Excised vesicles could be recognized from the anomalous, transient H^+ current activation upon depolarization and repolarization. On average >50% of all attempts resulted in high quality inside-out patch. PMA pretreatment, nucleotides in the bathing solution, and NBT in the pipette all lowered the success rate. For applying different bathing conditions two approaches were used. When complete solution change was required the chamber contained 150 μl of recording solution. Solution change was performed within ~1.5 min by infusing 1.5 ml of the desired solution from a gravity-driven perfusion system. The excess volume was continuously removed by a suction pump. When bath solutions contained ATP and GTP-γ-S the initial working volume was 50 μl and drugs, such as NADPH and DPI, were pipetted directly into the bath followed by thorough mixing (pipetting five times with a 20-μl pipette). Each drug application caused 1% error in the ATP and GTP-γ-S concentration, except for the case of 4 mM NADPH application, which caused 5% error. Experiments performed this way were finished within 30 min after the chamber was filled with the bath solution to avoid significant effect of evaporation. Washout of the nucleotides was achieved by perfusing 1 ml nucleotide free solution as described above. Voltage-clamp experiments were performed using Axoptach-1D patch-clamp amplifier (Axon Instruments, Inc.). Pipettes were pulled from borosilicate glass tubing (type GC150F-10; Clark Electromedical) using a P-87 puller (Sutter Instrument Co.). After fire polishing the tip the pipette resistance was 12–30 MΩ when filled with the pH 7.5 solution (composition see below). The resistance of the same pipettes ranged between 3–6 MΩ when filled with 150 mM KCl solution, indicating that the pipette tip had a size commonly used in whole-cell experiments (diameter ~1 μm). The bath was grounded using an Ag/AgCl pellet. Current data were not routinely corrected for leak unless it was an inherent result of the applied experimental or analytical approach, as described in the results section. Complete absence of H^+ or e^- current is stated when the measured current is not different from the leak current at a given voltage, as estimated from the holding current measured at a negative, sub-threshold membrane potential (usually −60 mV) in the nominal absence of NADPH. Current was low-pass filtered at 20–100 Hz (−3 dB, 8-pole Bessel filter) and digitally sampled at a rate at least 2.5 times the corner frequency of the analogue filter. For data analysis and figure preparation further, software-based (pClamp 8; Axon Instruments, Inc.) noise reduction was performed offline (simulating an 8-pole Bessel filter). Traces in figures are low-pass filtered offline at 5 Hz (−3 dB) unless otherwise specified in the figure legend. Experiments and data storage were performed using software pClamp 6 (Axon Instruments, Inc.), while for data analysis pClamp 8 was used, both running on a PC/AT computer. Online compensation for the full electrode capacitance was not performed, because the stable extent of electrode immersion could not be ensured after a solution change. Continuous current recordings in this paper were neither intended nor suited to perform tail-current analysis, therefore changes in tail-current kinetics are not interpreted, although in most cases they displayed the expected changes, based on earlier reports (see DISCUSSION for details).

Solutions

The cell storage media was a 2:1 mixture of Medium 199 with L-glutamine and L-amino acids containing 25 mM HEPES (GIBCO BRL) and L-glutamine free RPMI 1640 Medium (GIBCO BRL) supplemented with 5 mM Na_2EDTA and 2% fetal calf serum (BioConcept). The recording solutions contained (mM): CsCl 1, tetraethylammonium chloride 1, $MgCl_2$ 2, EGTA 1, N-methyl-D-glucamine base 101 and either 200 MES acid for pH 6.1 or 200 HEPES acid for pH 7.5. To establish pH 7.0 solution pH 7.5 and pH 6.1 solutions were mixed at a volume ratio of 3:2 (7.5 versus 6.1, respectively). Free [Zn^{2+}] was calculated using MaxChelator

software (version 2.10, http://www.stanford.edu/~cpatton/maxc.html, written by Chris Patton) and buffered with 3 mM citrate in the μM range or by the 1 mM EGTA in the nM range. Zinc effect was tested using citrate containing pH 7.5 solution, as HEPES does not bind Zn^{2+} significantly (Cherny and DeCoursey, 1999). The pH of citrate containing solution with 45 μM free Zn^{2+} was 7.43. Osmolality of the above recording solutions was in the range of 315–322 mosmol/kg, as measured with a freezing point osmometer. The osmotic and volume changes induced by bath application of different compounds were not corrected for. Li_4GTP-γ-S was dissolved in water at 10 mM. DPI was first dissolved in DMSO to give a 10-mM stock, which was then further diluted in pH 7.5 solution to 200 μM. PMA was dissolved in DMSO at 1 mM. MgATP and Na_4NADPH was dissolved in pH 7.5 solution to give a stock solution of 30 and 80 mM, respectively. $ZnCl_2$ was dissolved at 0.5 M in water containing 40 mM HCl. Na_2EDTA was dissolved in water at 250 mM. All chemicals were obtained from Sigma-Aldrich unless otherwise specified. All manipulations were performed on room temperature (23–25°C), unless otherwise stated.

Conventions

The sign of the originally recorded inside-out patch current signal is inverted in figures; thus, positive current value indicates outward current to comply with classical whole-cell experiments. Intracellular pH (pH_i) is the pH of the bath solution facing the cytoplasmic side of the excised patch membrane, while the pH of the pipette solution corresponds to pH_o (extracellular pH).

Data Analysis

The number of cells (n) indicates the cumulative number of measurements performed on at least two independent cell preparations. Data are presented as mean ± SD. For statistical analysis paired or unpaired Student's t test and ANOVA for repeated measures was applied using Statistica software (version 4.5; Statsoft, Inc.). For ANOVA post hoc comparisons the Tukey honest significant difference test was applied. A value of $P < 0.05$ was considered statistically significant. Linear regression and correlation coefficients were calculated using the built-in algorithm of Origin software (version 6.0; Microcal Software, Inc.). Exponential fit of current activation and its extrapolation were performed with the built-in algorithm of pClamp 8 software. For all fits and regressions the sum of squared error minimization method was applied.

Online Supplemental Material

Supplemental figures available online demonstrate the proton selectivity (Fig. S1) and DPI sensitivity (Fig. S4) of depolarization-activated inward current. Further figures depict the rundown of electron current in ATP- and GTP-free solutions (Fig. S2) and the correlation between inward and outward H^+ currents and between e^- and outward H^+ currents (Fig. S3). These measurements were performed in patches excised from PMA-treated eosinophils. Online supplemental material is available at http://www.jgp.org/cgi/content/full/jgp.200308891/DC1.

RESULTS

Proton Currents in Inside-out Patches from Nonstimulated Eosinophils

In most patches excised from slightly adherent, but otherwise not stimulated human eosinophils a depolarization-induced, noninactivating current was observed at positive membrane potentials (Fig. 1 A, $n > 50$). The activation kinetics and steady-state amplitude of the depolarization-activated current displayed only very moderate changes over the 5–15-min recording period and moderate, spontaneous current run-down was infrequently observed. The activation of outward current was extremely slow, typically requiring more than 1 min to reach steady-state current amplitude at 80 mV (inside positive) when a symmetrical pH of 7.5 was maintained on both sides of the membrane. The steady-state current amplitude at 80 mV was 6.7 ± 2.6 times larger when pH_i was 6.1 instead of 7.5 ($n = 6$, $P < 0.003$, Fig. 1 B). The steady-state current displayed excess fluctuation at 80 mV in the low frequency bandwidth (<10 Hz) as compared with the background noise measured at −80 mV (Fig. 1 C). Occasionally, slowly gating single-channel events could be observed that superimposed the depolarization-activated current (Fig. 1 A). The two phenomena were not related, as single-channel events could also be observed at negative E_m and had an apparent reversal potential of 0 mV under all $pH_{i/o}$ conditions.

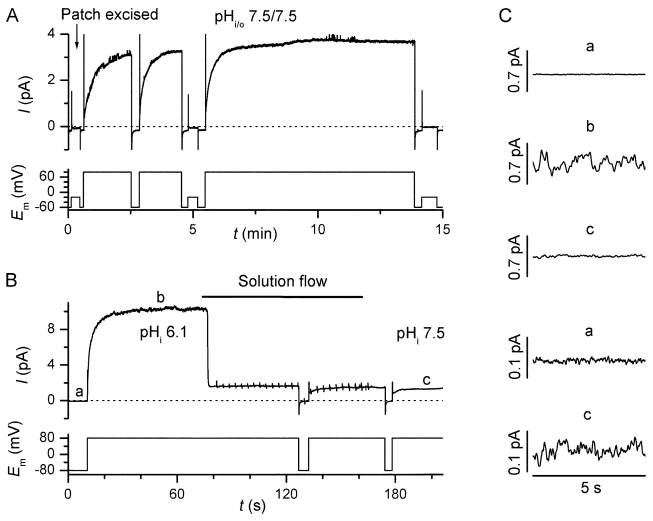

FIGURE 1. Depolarization-activated, pH_i-sensitive currents in inside-out patches from nonstimulated human eosinophils. Human eosinophils were adhered to glass coverslips in the absence of soluble stimuli and patched within 10 min of plating. (A) After patch excision at −20 mV (arrow) depolarization to 80 mV evoked time-dependent currents that activated slowly and were stable for several minutes. The voltage protocol is displayed below the current traces. (B) Effect of bath alkalization from pH 6.1 to 7.5 on the current amplitude at 80 mV. Spikes on the current trace during solution change are capacitance artifacts caused by the suction pump. Trace is representative from six experiments with similar results. (C) Excess fluctuations associated with the outward current (b and c), are compared with the background noise measured at $\sim E_H$ (a). Traces a and c are shown of two different scales to match the steady-state current amplitude measured at pH_i 6.1. Time bar applies to all traces in C.

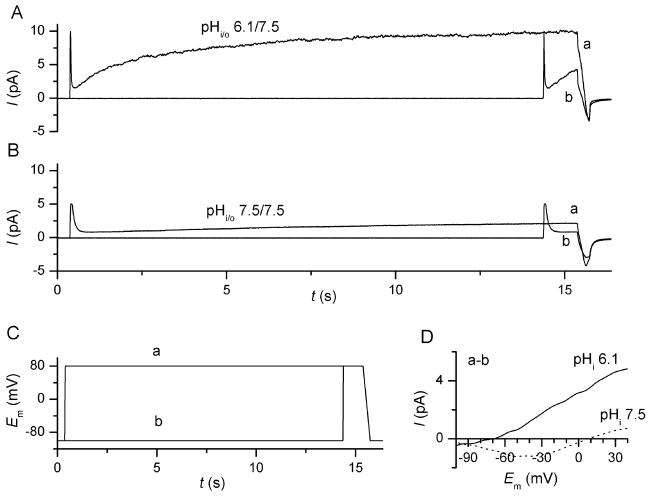

FIGURE 2. Effect of pH_i change on E_{rev}. To determine the reversal potential (E_{rev}) of the depolarization-activated current, we took advantage of its slow activation kinetic. Every 25 s, a long-lasting (15 s, a) or short-lasting (1 s, b) activating pulse to 80 mV was applied, followed by a rapid voltage ramp to the −100-mV holding potential (C). This voltage protocol was applied at different transmembrane pH gradients (A and B), and the reversal potential of the voltage- and time-dependent currents (D) was determined by subtracting the two "ramp tail" currents (a − b). Increasing the pH_i from 6.1 to 7.5 caused an ~75-mV shift in the 0 current potential (E_{rev}). Traces are low-pass filtered at 30 Hz and are representatives of six experiments with similar results.

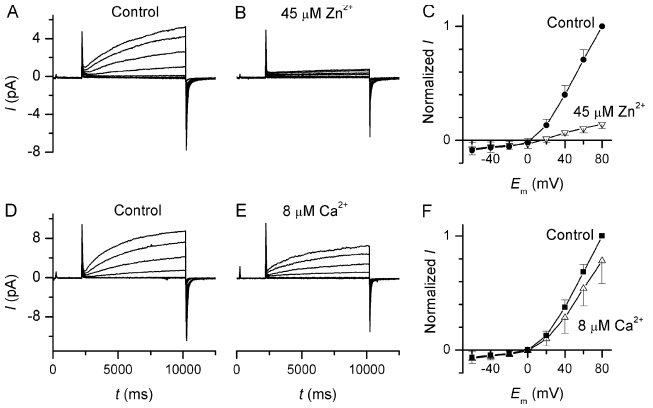

FIGURE 3. Effects of intracellular Zn^{2+} and Ca^{2+} on the proton currents. Voltage steps were applied every 15 s from the −80 mV holding potential to −70 mV and then to test potentials ranging from −60 to 80 mV in 20-mV increments. Current traces were acquired under control conditions (A and D) or in the presence of 45 μM free Zn^{2+} (B) or 8 μM Ca^{2+} (E). Traces were low-pass filtered at 20 Hz, $pH_{i/o}$ was 7.43–7.47/7.5, citrate concentration in the bath was 3 mM in all cases. (C and F) Effect of 45 μM Zn^{2+} ($n = 5$, ●, control; ▽, Zn^{2+}) and 8 μM Ca^{2+} ($n = 4$, ■, control; △, Ca^{2+}) on the near steady-state current-voltage relationship. The average current during the last second of the 8-s long voltage step was measured at different test potentials. The measured current amplitudes at each test potential were normalized to the control value measured at 80 mV in the same patch. Time scale applies to all current traces. Traces in A and B and D and E have the same current scale.

To assess the ionic selectivity of the currents, we analyzed the reversal potential (E_{rev}) of the depolarization-activated current using "ramp-tail" protocols (Fig. 2). The E_{rev} measured at a symmetrical pH of 7.5 was 0.5 ± 4.8 mV (estimated E_H 0 mV). Acidifying the internal pH to 6.1 (estimated E_H −82.4 mV) caused a −77.2 ± 5.5 mV shift in E_{rev} (Fig. 2 D, $n = 6$, $P < 10^{-6}$). This value indicates a mean of 54.4 mV/pH unit change in reversal potential, which is in good agreement with the theoretical Nernstian slope of ~58 mV/pH unit, at ~25°C for a purely H^+-selective conductance. The above data indicate that the charge carrier of the depolarization-activated current is H^+ and that the current is carried by slowly gating, small conductance proton channels.

H^+ Currents Are Inhibited by Internal Zn^{2+}

Among extracellularly applied polyvalent cations Zn^{2+} proved to be the most potent inhibitor of voltage-dependent H^+ currents (DeCoursey, 2003). Data available on human eosinophils indicate that the effect of extracellular Zn^{2+} is voltage and pH dependent. The extracellular application of Zn^{2+}, at free concentrations ranging from 10 to 50 μM, induces complete or near complete block of outward H^+ currents (Gordienko et al., 1996; Schrenzel et al., 1996; Banfi et al., 1999) under varying voltage (60–80 mV) and pH_o (7.0–7.5) conditions. To test whether intracellular Zn^{2+} can have a similar inhibitory effect on H^+ currents, we applied ~45 μM free Zn^{2+} at pH_i 7.5 (Figs. 3, A–C). We found that the near steady-state H^+ current amplitude was reduced to 30 ± 8.9% ($n = 6$, $P < 10^{-5}$) at the end of an 8-s long voltage step to 60 mV. The average, uncorrected chord conductance was reduced by 8.4-fold between 20 and 40 mV and by 23.4-fold between 60 and 80 mV. This indicates that the Zn^{2+} effect is voltage dependent and that inhibition is more pronounced at depolarized potentials. The inhibitory effect of Zn^{2+} was, however, only partially reversible in five out of six cases.

As the affinity of metal chelators for Zn^{2+} is often much higher than that for Ca^{2+} or Mg^{2+}, we examined the possibility that liberation of Ca^{2+} and Mg^{2+} from the chelators (EGTA and citrate) by Zn^{2+} could account for the reduction in H^+ current. For this purpose, we tested the effect of ~8 μM free Ca^{2+}, buffered with 3 mM citrate. The influence of micromolar free Ca^{2+} on the near steady-state H^+ current amplitude ranged from no effect to 23% reduction (at 60 mV, $n = 4$, $P > 0.9$, Fig. 3, D–F). In the latter cases however, the decrease in H^+ current amplitude was completely irreversible, suggesting that Ca^{2+} may induce irreversible run-down of the current. The average uncorrected

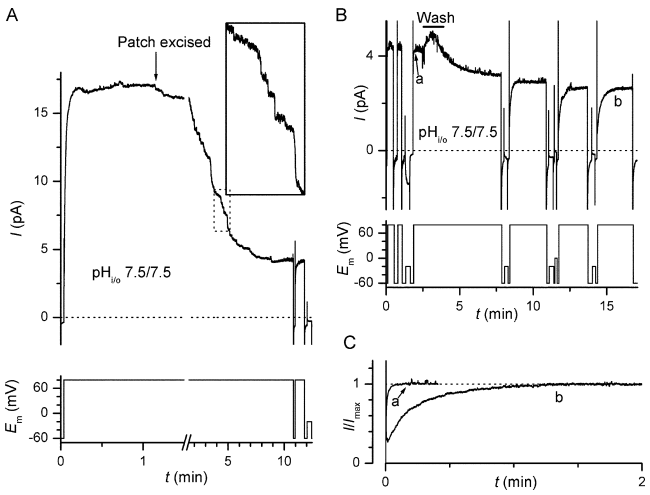

FIGURE 4. Proton current in patches excised from PMA-stimulated eosinophils. Human eosinophils were adhered to glass coverslips in the presence of 200–400 nM PMA and patched after 5–10 min of stimulation. (A) Progressive run-down of H^+ current could be observed when patches were excised (arrow) into ATP and GTP-γ-S–free bath solution. Stepwise changes with unexpectedly large amplitude (insert) were present in the course of run-down in 14 of 16 patches excised into nucleotide-free solution. Note the break in the time axis. (B) Absence of run-down in a patch excised in a bath solution containing 3 mM ATP and 20 μM GTP-γ-S. When indicated, the bath was exchanged to a nucleotide-free solution. The increase in H^+ current amplitude during solution flow probably reflects the mechanosensitivity of H^+ channels in the excised patch (unpublished data). Trace is representative of six experiments with similar results. In one case stepwise changes were observed after washing out the nucleotides. (C) Currents from B elicited by a pulse to 80 mV were normalized to the steady-state current amplitude to demonstrate the difference between the activation kinetics before (a) and after (b) run-down.

chord conductance was reduced by 1.32-fold between 20 and 40 mV and by 1.30-fold between 60 and 80 mV, indicating that the Ca^{2+} block is not influenced by the membrane potential.

The reversibility of the Zn^{2+} block could be tested directly in cell patches sequentially exposed to different Zn^{2+} concentrations. Shifting from ~100 nM to ~3 μM Zn^{2+} reduced the amplitude of the steady-state H^+ current by 69 ± 6.5% (at 80 mV, $n = 4$, $P < 0.0005$), whereas subsequent application of ~45 μM Zn^{2+} eliminated any depolarization-activated H^+ current within 3 min at 80 mV. These effects were completely reversible.

Proton Current in Excised Patches from PMA-stimulated Eosinophils

PMA is a well-known activator of the phagocytic NADPH–oxidase and of its related proton channel (DeCoursey et al., 2000, 2001). When patches were excised from eosinophils pretreated with supramaximal stimulatory doses of PMA (200–400 nM for 5–10 min), membrane depolarization also activated an outward current in the vast majority of patches ($n > 50$). The kinetic of activation was, however, much faster than in nontreated patches as steady-state was usually reached within 20 s (Fig. 4 C). This finding is in qualitative agreement with earlier reports that compared the characteristics of whole-cell H^+ currents in activated and nonactivated phagocytes (Banfi et al., 1999; DeCoursey et al., 2000, 2001). Unlike whole-cell currents, however, H^+ currents in inside-out patches were subject to progressive run-down, which started within 3 min after patch excision and usually stopped within 10 min (Fig. 4 A). Unexpectedly, stepwise reductions in current amplitude were regularly observed during run-down (14 of 16 cells, Fig. 4 A, inset). The run-down could be strongly hampered or completely blocked by bath application of 3–5 mM ATP and 20–25 μM GTP-γ-S, while washing out these compounds initiated run-down within <1 min (Fig. 4 B). The run-down never resulted in the complete loss of outward H^+ current, but instead reverted its activation kinetic and long-term stability to those observed in nonactivated cells (Fig. 4 C).

Besides faster activation kinetics, cells with an active oxidase display a strong negative shift (by ~40 mV) in the H^+ current threshold potential,[1] which allows inward H^+ current under certain pH conditions (Banfi et al., 1999; DeCoursey, 2003). This feature is considered the hallmark of H^+ channels associated with an active oxidase, as in other cell types, in nonactivated phagocytes, and also in eosinophils from CGD patients the H^+ currents are otherwise strictly outward (Banfi et al., 1999; DeCoursey, 2003). We therefore sought inward proton currents in patches excised from PMA-stimulated cells by applying depolarizing voltage steps to −20 mV at $pH_{i/o}$ 7.5/7.5 ($E_H = 0$ mV, Fig. 4 B) or to 0 mV at $pH_{i/o}$ 7.5/7.0 ($E_H = 29$ mV, Fig. 5). As shown in Figs. 4 B and 5, time-dependent inward currents could be evoked under these circumstances. These inward currents invariably displayed complete run-down in ATP and GTP-γ-S–free solutions (Fig. 4 B), while in the presence of ATP and GTP-γ-S run-down could be completely prevented in some cases. The run-down occurrence could be minimized further by using larger pipettes to excise larger patches. As shown in Figs. 4 B and 5, the run-down of inward and outward currents were strictly correlated. Both inward and outward currents were carried by H^+ ions, as the average reversal potential of the time-dependent inward currents determined by ramp-tail measurements was 31 ± 2.3 mV at $pH_{i/o}$ 7.5/7.0 ($E_H = 29$ mV, Fig. S1, available at http://

[1]The empirical equations that can be applied to estimate the H^+ current threshold potential ($E_{threshold}$) under different E_H (E_{rev}) conditions in resting and PMA treated eosinophils are $E_{threshold} = 0.79\ E_{rev} + 23$ mV and $E_{threshold} = 0.63\ E_{rev} - 22$ mV, respectively (DeCoursey, 2003).

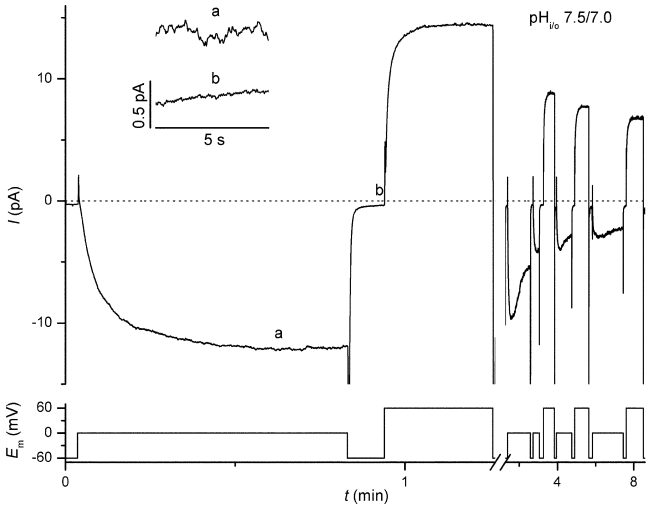

FIGURE 5. Properties and run-down of inward and outward H^+ currents. Patches excised from PMA stimulated eosinophils were recorded in a bath solution containing 5 mM ATP and 25 μM GTP-γ-S. Inward and outward H^+ currents were elicited by pulses to 0 and 60 mV, the driving forces for H^+ current at these voltages were approximately −30 and 30 mV, respectively. In every patch exhibiting run-down, the two currents decreased in parallel ($n >$ 20). Note the break in the time axis. Inset demonstrates excess low-frequency fluctuations associated with the inward H^+ current recorded at 0 mV (a) as compared with the background noise recorded at −60 mV (b). Time and current bars apply for both traces in the insert.

www.jgp.org/cgi/content/full/jgp.200308891/DC1), while in the same patches E_{rev} of the outward currents was 30.4 ± 2.8 mV ($n = 9$). Because of the small amplitude of the inward currents no such test could be applied in symmetrical pH conditions (pH$_{i/o}$ of 7.5/7.5), where E_H was 0 mV. However, depolarization activated inward and outward currents were present at −20 and 20 mV, respectively, whereas no or very small current could be measured at 0 mV (unpublished data), indicating that E_{rev} was ∼0 mV under these conditions. At pH$_{i/o}$ 7.5/7.0 excess low-frequency fluctuations were also associated with the inward proton current activation at 0 mV (Fig. 5, inset).

Electron Current in Excised Patches from PMA-pretreated Cells

The activity of NADPH–oxidase can be measured electrically (electron currents) and chemically ($O_2^{\cdot -}$ production) at the single-cell level using the patch-clamp technique and the NBT test, respectively (Schrenzel et al., 1998; Banfi et al., 1999). We thus wondered whether these activities could be detected in excised patches from PMA activated eosinophils. For this purpose, we included 5 mM ATP and 25 μM GTP-γ-S in the bath solution, as earlier reports indicate that these compounds help to maintain oxidase activity (Schrenzel et al., 1998; Banfi et al., 1999; Moskwa et al., 2002; Brown et al., 2003). As shown in Fig. 6 A, under these conditions bath application of 4 mM NADPH evoked sustained inward current at −60 mV, a voltage at which H^+ channels are essentially closed (pH$_{i/o}$ 7.5/7.0). This current was completely blocked within 5 min by bath application of 2 μM DPI, an organic inhibitor of the phagocytic NADPH–oxidase (Doussiere and Vignais, 1992; Schrenzel et al., 1998; Banfi et al., 1999; Doussiere et al., 1999). When patches were excised into ATP- and GTP-γ-S–free bath solution, the NADPH-evoked inward current progressively ran down, with a time course comparable to that of the H^+ current run-down under the same conditions, but without stepwise changes (Fig. S2, available at http://www.jgp.org/cgi/content/full/jgp.200308891/DC1). Inclusion of 0.5 mg/ml NBT in the patch pipette allowed us to directly detect the production of $O_2^{\cdot -}$ at the surface of the membrane patch, as NBT reduction led to the formation of dark formazan precipitates within the pipette tip (Fig. 6 B). In the presence of extracellular (pipette) NBT, bath application of 0.8 mM NADPH evoked an inward current, which progressively decreased with time (Fig. 6 C). This decrease almost certainly reflected the clogging of the pipette tip by the $O_2^{\cdot -}$-induced NBT precipitates, as under these conditions not only the electron current, but also inward and outward H^+ currents became undetectable, a scenario that was otherwise never observed. Interestingly, in the presence of NBT stepwise changes were observed in four out of seven patches during e^- current fade-out, possibly reflecting a clustered distribution of oxidase functional units in the membrane (Nugent et al., 1989; Wientjes et al., 1997). These experiments indicate that both electron currents and superoxide production can be measured in inside-out patches from PMA-stimulated eosinophils, confirming the presence of an active NADPH–oxidase.

Relationship between Proton and Electron Currents

The intimate connection between NADPH–oxidase activity and H^+ current activity in phagocytes is widely accepted. The connection is so close that it led to the proposal that the membrane subunit of the oxidase, gp91^{phox}, comprises a built-in H^+ pathway (channel) that accounts for most of the currents observed in activated phagocytes (Henderson, et al., 1995; Banfi et al., 1999). Recent data, however, strongly challenge the notion that gp91^{phox} is a proton channel (for review on the debate consult the following perspectives: DeCoursey et al., 2002; Henderson and Meech, 2002; Touret and Grinstein, 2002; Maturana et al., 2002). The use of inside-out patches allowed us to reassess two pieces of evidence against the channel nature of gp91^{phox} that were obtained by whole-cell perforated patch measurements in PMA activated human phagocytes: (a) the lack of correlation between the amplitude of H^+ and e^- currents

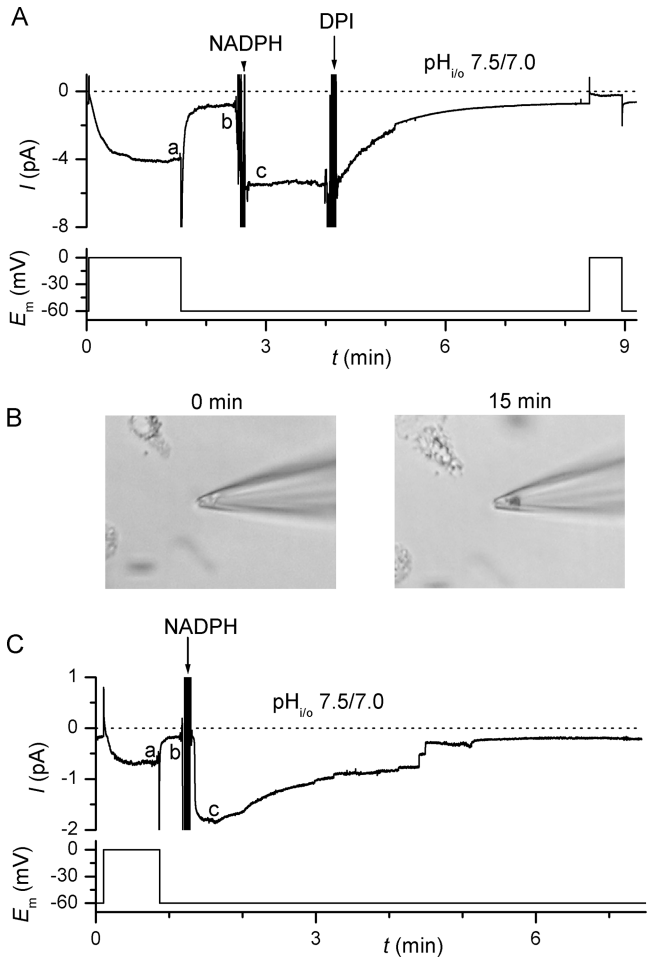

FIGURE 6. Electron currents and superoxide production in patches excised from PMA-treated eosinophils. (A) Bath application of 4 mM NADPH (arrowhead) evoked an electron current at −60 mV that was blocked by 2 μM DPI (arrow). (B) A patch excised with a pipette containing 0.5 mg/ml NBT was photographed shortly before (left) and 15 min after (right) bath application of 0.8 mM NADPH. Note the formation of a dark NBT precipitate (formazan) due to $O_2^{\cdot -}$ production near the pipette tip. The patch was excised from the cell at 11 o'clock from the pipette tip. (C) The e^- current evoked by 0.8 mM NADPH (arrow) in the presence of 0.5 mg/ml pipette NBT faded out with time in a stepwise manner. Traces are representatives of the experiments used to establish $I_e - I_H$ plots (Fig. 7), in which the amplitude of the inward H^+ current was measured at 0 mV just before stepping back to −60 mV (a), whereas the e^- current was measured as the difference between the holding current amplitude at −60 mV in the absence and presence of NADPH (b and c).

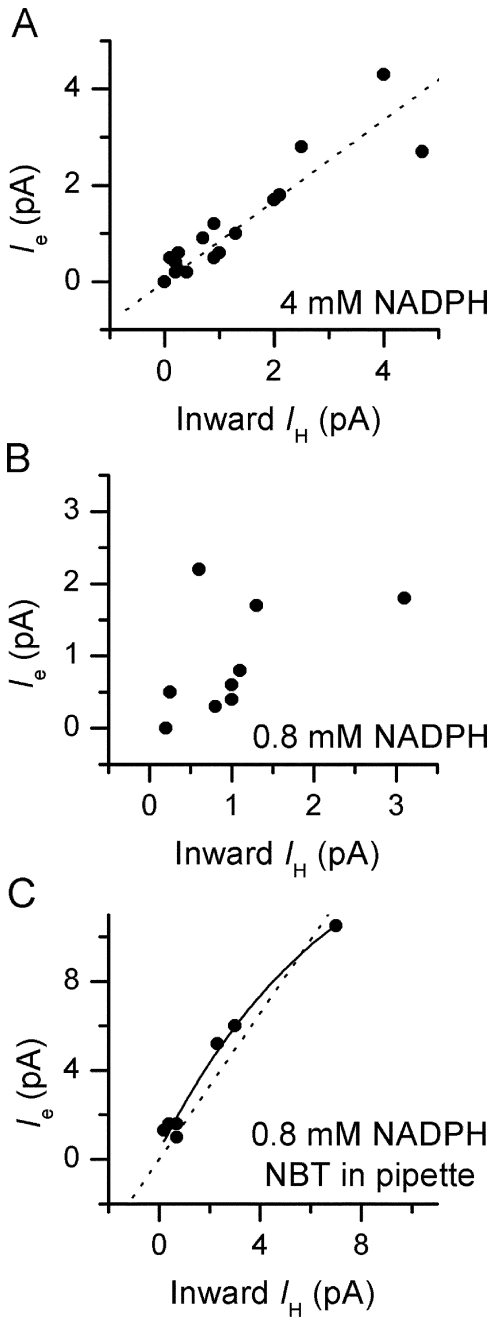

FIGURE 7. Correlation between inward H^+ and e^- currents. Proton and electron currents were evoked and measured as described in Fig. 6. Electron currents were induced either by bath application of 4 mM (A) or 0.8 mM NADPH in the absence (B) or presence (C) of 0.5 mg/ml NBT in the pipette solution. Steady-state (A and B) or peak (C) e^- current amplitudes at −60 mV are plotted against the average inward H^+ current amplitude during the last 5 s at 0 mV. Dotted lines are the results of linear regressions constrained to pass through the origin ($R > 0.91$ for panel A and $R > 0.98$ for panel C). Solid line in C is the result of fitting a first order decaying exponential curve to the data ($R^2 > 0.98$) to demonstrate apparent saturation of electron transport, probably reflecting the limitation in electron current amplitude due to NBT precipitation.

(DeCoursey et al., 2000), and (b) the lack of effect of the oxidase-specific blocker DPI on PMA-activated H^+ currents (DeCoursey et al., 2000, 2001). As shown in Fig. 7, a correlation could be observed between the amplitude of inward H^+ and e^- currents in excised patches. The inward H^+ current was measured at 0 mV shortly before the addition of NADPH (pH$_{i/o}$ 7.5/7.0) and the e^- current was taken as the difference between the holding current amplitude measured at −60 mV in the

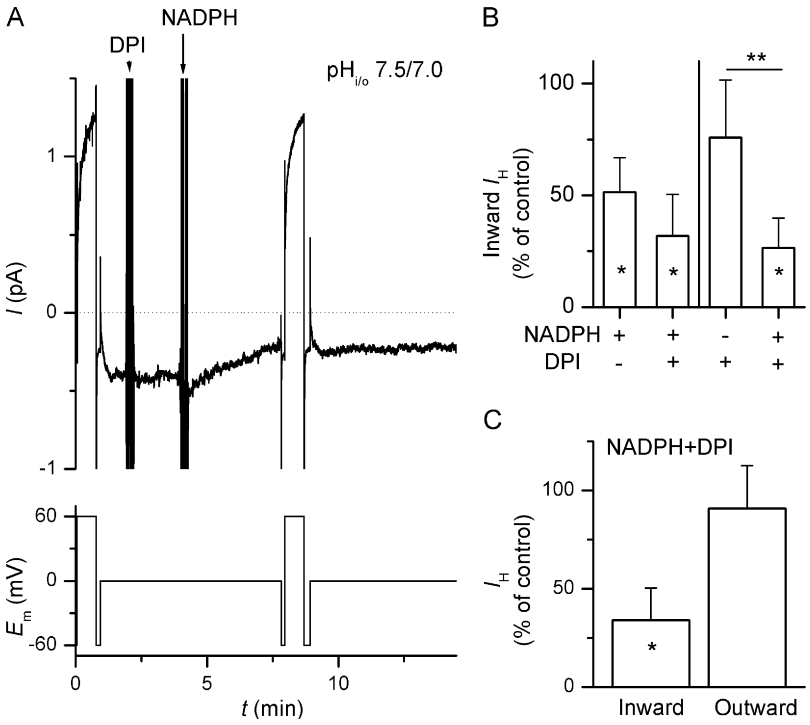

FIGURE 8. Effects of DPI and NADPH on the proton current. (A) Effect of sequential bath application of 2 μM DPI (arrowhead) and 0.8 mM NADPH (arrow) on inward and outward H^+ currents. Note the transient increase in the inward current amplitude preceding the inhibition of the H^+ current after the application of NADPH. The patch was excised from a PMA-treated cell. The bath solution contained 5 mM ATP and 25 μM GTP-γ-S. (B) Summary of the effect of 2 μM DPI and 0.8 mM NADPH on the inward H^+ current with NADPH or DPI added first (left and right, respectively, $n = 5$ each). Single asterisks denote significant difference from control values, double asterisk indicates significant difference between columns. (C) Summary of the combined effect of 2 μM DPI and 0.8 mM NADPH on the inward and outward H^+ current ($n = 7$). Data are compiled from Fig. 8 B, irrespective of the sequence of addition. Asterisk indicates significant difference from control values. To remove the potential contribution of e^- currents, a biexponential fit was applied to the depolarization-activated H^+ currents, extrapolated to the zero and steady-state values (for the 60-mV pulse only), and the difference taken as H^+ current amplitude.

absence and presence of NADPH (Fig. 6 A, a, c–b). The two parameters correlated very well when 4 mM NADPH was applied to the bath to elicit the e^- current (Fig. 7 A, $R > 0.91$ at $P < 10^{-4}$). No correlation was observed when a five times lower concentration of NADPH was applied (Fig. 7 B, $P > 0.3$ for the best fit of $R < 0.52$), unless NBT was added to the pipette to scavenge the reaction product, $O_2^{\cdot -}$ (Fig. 7 C, $R > 0.98$ at $P < 0.0002$).[2] A correlation was also observed between inward and outward H^+ currents in the absence of NADPH ($R > 0.71$ at $P < 0.001$, Fig. S3 A, available at http://www.jgp.org/cgi/content/full/jgp.200308891/DC1) and between outward H^+ and e^- currents evoked by 4 mM NADPH ($R > 0.70$ at $P < 0.002$, Fig. S3 B).

We next assessed whether DPI or NADPH, alone or in combination, had any effect on H^+ currents. For this purpose, only patches with stable inward currents were used (>30 s) to minimize the influence of H^+ current run-down on the DPI and NADPH effects. Fig. 8 A shows the effects of sequential addition of 2 μM DPI and 0.8 mM NADPH on the inward current measured at 0 mV and on the outward current measured at 60 mV. As summarized in Fig. 8, B and C, bath application of 0.8 mM NADPH significantly reduced the inward H^+ current amplitude, to 51.4 ± 14.4% ($n = 5$, $P < 0.0005$). DPI, on the other hand, had either no effect or induced up to 52.4% inhibition when applied alone (on average 75.8 ± 25.8%, $n = 5$, $P > 0.079$). Interestingly, when DPI had an inhibitory effect the reduction in H^+ current amplitude was often preceded by a transient inward current peak (Fig. S4, available at http://www.jgp.org/cgi/content/full/jgp.200308891/DC1), strongly resembling the phenomenon that was observed when NADPH was applied in the presence of DPI (Fig. 8 A). The strongest reduction could be observed when both DPI and NADPH were present (to 34 ± 16.3%, $n = 7$, $P < 10^{-4}$), independently of the sequence of application. The inhibition was specific for the inward H^+ currents, as in the same patches the outward H^+ current amplitude was not affected (91.8 ± 21.7% of control, $P > 0.3$). This not only implies that the DPI effect is specific for the inward current, but also indicates that the run-down was negligible in these conditions.

[2]The ability of NBT to capture electrons directly from the oxidase (Briggs et al., 1975) might also account for the increased correlation and larger e^- currents observed in the presence of NBT.

DISCUSSION

This study is the first to report parallel measurements in inside-out patches of electron and protons currents associated with a functional NADPH–oxidase. This methodological breakthrough, which opens the way to cell-free studies of the oxidase in its native membrane environment, allowed us to obtain new information on the function of the phagocytic NADPH–oxidase and its related proton channel.

Proton Currents from Nonstimulated Eosinophils and the Effect of Internal Zn^{2+}

In most patches excised from nonstimulated eosinophils, voltage-activated H^+ currents could be measured

and were the predominant currents observed. The current amplitude and its long-term stability were sufficiently large to perform a functional and pharmacological characterization of the underlying channel, under conditions that allow a stringent control of the pH on both sides of the membrane. The properties of the H^+ currents recorded in excised patches were consistent with earlier studies on phagocytic H^+ currents performed at the whole-cell level: voltage and pH dependency, exceptionally high selectivity for H^+, and direct activation by micromolar arachidonic acid (unpublished data; Kapus et al., 1994; Gordienko et al., 1996; Schrenzel et al., 1996, for review on the characteristics of phagocytic and other H^+ currents see DeCoursey, 2003).

The ability to apply agents from the internal side of the membrane allowed us to study the mode of action of Zn^{2+}, which inhibits H^+ currents in all cell types at submillimolar concentrations when applied from the external side (DeCoursey, 2003). In nonactivated eosinophils, a near complete block is achieved with a few 10 μM free extracellular Zn^{2+} (Gordienko et al., 1996; Schrenzel et al., 1996; Banfi et al., 1999), but it is unclear whether the Zn^{2+} binding sites are located on the extracellular side of the channel or even on the channel itself. In one study, the effect of extra- and intracellular Zn^{2+} were compared in rat alveolar epithelial cells. Only a moderate inhibition was observed at high intracellular Zn^{2+} concentrations (~170 μM), values much higher than those required for extracellular block at the same pH of 6.5 (Cherny and DeCoursey, 1999). The authors concluded that Zn^{2+} probably has a qualitatively and quantitatively different effect after external or internal application. This appears not to be the case in eosinophils, as a near complete block could be observed at an intracellular free Zn^{2+} concentration of 45 μM, while 3 μM internal Zn^{2+} caused more than half maximal inhibition of the steady-state H^+ current at 80 mV and pH_i 7.5. These data are comparable to that of Schrenzel et al. (1996), who tested the effect of external Zn^{2+} in human eosinophils and reported a half-inhibitory concentration of 4 μM at pH_o 7.5 (Schrenzel et al., 1996). Whether the apparent difference in Zn^{2+} action between epithelial cell and eosinophil is of methodological or biological origin is yet to be elucidated. Nonetheless, our data suggest that, in nonstimulated human eosinophils, the blocking action of Zn^{2+} is largely independent of its site of application with the notable exception that, contrary to extracellular application (Cherny et al., 2001), depolarization promotes the block by internal Zn^{2+}. Therefore, Zn^{2+} either binds to the same site(s) accessible from both sides of the membrane or to distinct intra- and extracellular sites that are still located within the membrane electrical field. We did not test the influence of pH_i on the inhibitory potential of Zn^{2+}, but as most sites that bind Zn^{2+} do bind proton similarly well, a pH_i decrease would probably diminish Zn^{2+} inhibition as observed with extracellular Zn^{2+} (DeCoursey, 2003).

Characteristics and Run-down of Proton Currents in Cells Stimulated with PMA

Earlier whole-cell patch-clamp measurements in phagocytes expressing a functional oxidase consistently show that proton currents have larger amplitude, lower threshold, faster activation, and slower deactivation kinetics when cells are stimulated with GTP-γ-S or PMA to activate the oxidase (Banfi et al., 1999; DeCoursey et al., 2000, 2001). The approximately −40-mV shift in the threshold potential (Banfi et al., 1999; DeCoursey et al., 2001) allows the influx of H^+ through the channel under appropriate pH conditions (Banfi et al., 1999), a unique condition among proton channels. Our results from inside-out patches confirm and extend these earlier reports. Large, rapidly activating inward H^+ currents could be induced by depolarizing voltage steps in patches excised from cells stimulated with PMA (Fig. 5). In the absence of NADPH the inward and outward H^+ currents were of similar amplitude when measured at an identical H^+ driving force, and were both associated with excess current fluctuations (Fig. 5). Interestingly, this phenotype ran down within minutes in patches excised from PMA-treated cells, although run-down could be hampered by adding ATP and GPT-γ-S to the cytosolic side of the patch. The run-down resulted in a partial loss of outward current amplitude, slowing of the activation kinetic, and complete loss of inward H^+ currents. In many cases (e.g., Fig. 4 B) only a single kinetic component was observed when outward H^+ currents were elicited at the beginning of the recording and after run-down had stopped. This suggests that the run-down reflects the transition between two functional state of the same channel, as was proposed by others for PMA stimulation (DeCoursey et al., 2001). Thus, contrary to our earlier proposal based on recordings of eosinophils from CGD patients (Banfi et al., 1999), normal eosinophils appear to express only one type of H^+ channels.

Unexpectedly, the run-down often occurred in an abrupt, stepwise manner. The amplitude of the current steps far exceeded the current size that can be carried by a single H^+ channel based on current fluctuation analysis or theoretical considerations (see below), suggesting that these abrupt transitions do not reflect the closing of single proton channels. One possibility is that the stepwise current changes reflect the pinch-off of membrane vesicles from the patch. However, this possibility appears unlikely as vesicle formation and detachment are energy-requiring processes, while the stepwise run-down often began to occur minutes after excising the patch and was observed preferentially in

the absence of ATP and GTP. Another possible explanation is that proton channels are clustered in the plasma membrane and display state transitions in a concerted manner, as was shown for many other ion channels (Schindler et al., 1984; Hymel et al., 1988; Geletyuk and Kazachenko, 1989; Schreibmayer et al., 1989; Marx et al., 1998; Bukauskas et al., 2000; Wang et al., 2000; Tanemoto et al., 2002). Cooperation between H^+ channels or channel subunits may also explain the delay and sigmoidicity in the channel activation kinetic that is observed in phagocytes and in alveolar epithelial cells (DeCoursey, 2003).

The run-down phenomenon provided new evidence linking electron transport to proton channel activity. Both electron and proton currents ran-down with similar kinetics (Fig. S2), and stepwise changes were also observed during electron current fade-out when NBT was present in the pipette (Fig. 6), consistent with clustering of both entities. In addition, the run-down of both proton and electron currents could be partially, and sometimes fully, inhibited by the simultaneous presence of internal ATP and GTP-γ-S. These nucleotides are required to maintain the oxidase activity in cell free systems (Ligeti et al., 1988; Doussiere and Vignais, 1992) or in streptolysin-O permeabilized phagocytes (Brown et al., 2003). High concentrations of ATP may be required to maintain the phosphorylation pattern of the oxidase subunits (Babior et al., 2002) and/or of membrane phospholipids such as phosphoinositides (Kanai et al., 2001; Karathanassis et al., 2002; Brown et al., 2003; Stahelin et al., 2003). ATP and GTP, on the other hand, are required to maintain the activity of several ion channels in excised patches. The observation that ATP and GTP-γ-S are required to maintain the activity of both electron and proton current in excised patches indicates that the these nucleotides modulate the underlying transport proteins in a similar way. Because GTP-γ-S has been shown to bind directly to membrane associated small GTP-ases within the activated phagocytic oxidase complex (Bokoch and Diebold, 2002), it is tempting to speculate that the proton channel is also part of the oxidase complex. Alternatively, the channel and oxidase might be separate entities sharing a very similar regulation. This is not unexpected, as prolonged function of the oxidase relies on H^+ channel activity (Kapus et al., 1993; Banfi et al., 1999; DeCoursey et al., 2003). Further experiments are required to understand the inactivation process underlying the run-down phenomenon and to determine the site of actions of the nucleotides.

Low-frequency Noise Associated with Proton Current

The depolarization activated H^+ currents are thought to be carried by voltage-gated proton channels. One of the fundamental arguments that the current is flowing through channels rather than carriers is the presence of excess fluctuation during current activation (DeCoursey, 2003). These fluctuations are thought to denote abrupt transitions between conducting and nonconducting states of the channel, called gating events (Hille, 1992). Based on statistical considerations, the average conductance of the underlying single channel can be calculated from the measured average macroscopic H^+ current amplitude, its variance, and estimated open probability (Hille, 1992). In patches excised from nonstimulated eosinophils a characteristic increase in current noise could be observed in the low-frequency bandwidth (<10 Hz) during outward H^+ current activation (Fig. 1), consistent with a recent study (Cherny et al., 2003). Our observation that steady-state inward H^+ current from activated eosinophils also display similar fluctuation at 0 mV, where no other significant noise source is present (Fig. 5), leaves hardly any doubt that these fluctuations are produced by state transitions of H^+ channels. Surprisingly, the estimated single H^+ channel conductance derived from these fluctuations (~30–140 fS, Cherny et al., 2003) is at least an order of magnitude larger than predicted if H^+ diffusion in the bulk solution was rate limiting. Several hypotheses were proposed to resolve this apparent contradiction, the discussion of which exceeds the scope of this paper (for review see DeCoursey, 2003). A simpler but as yet not considered explanation might be that H^+ channels are in fact clustered, as mentioned above, and might function (gate) in concert.

Relationship between Proton and Electron Currents

There is an ongoing debate about the channel nature of the core subunit of the phagocytic NADPH–oxidase, $gp91^{phox}$, which has been proposed to possess a built-in H^+ pathway (Henderson et al., 1995; Banfi et al., 1999). Unfortunately, this study cannot provide a definite answer as to the identity of the proton channel molecule, but using the inside-out patch approach we could challenge two earlier results obtained at the whole-cell level. In the first series of experiments we tested whether H^+ and e^- current amplitudes are correlated. No correlation was observed in whole-cell perforated patch measurements between the amplitudes of e^- current and of the maximal outward H^+ conductance in cells stimulated with PMA, arguing against the H^+ channel nature of the oxidase (DeCoursey et al., 2000). Because outward H^+ currents are observed regardless of the activation state of the oxidase, we initially investigated the relationship between e^- and inward H^+ currents. Like e^- currents, the presence of inward H^+ current depend on the assembly of oxidase complex, which shifts the voltage threshold of H^+ channel activation below E_H (Banfi et al., 1999). We could observe a good correlation between inward H^+ and e^- currents

at saturating concentrations of the substrate, NADPH, or when the reaction product, $O_2^{\cdot -}$ was rapidly removed from the extracellular side by a scavenger. Under these conditions, the driving force for e^- across the patch of membrane (redox potential difference calculated from the NADPH:$NADP^+$ and O_2:$O_2^{\cdot -}$ ratios at a given pH) is expected to remain relatively constant. In contrast, at lower [NADPH] and without an external $O_2^{\cdot -}$ scavenger the steady-state O_2:$O_2^{\cdot -}$ ratio at the extracellular membrane surface might strongly depend on the number of active oxidases in the patch, as the pipette tip is a limited diffusion space. This might account for the lack of correlation observed with 0.8 mM NADPH (Fig. 7 B). Similarly, the lack of correlation reported in whole-cell studies might reflect cell to cell variations in the metabolic state, as the intracellular concentration of NADPH cannot be controlled in perforated patch measurements (DeCoursey et al., 2000). The correlation that we observed in excised patches did not depend on the direction of the H^+ flux, as a linear correlation was also observed between the amplitude of e^- currents and the amplitude of the outward H^+ currents measured in the same patch.

The correlation indicates that the two functions are coupled, but does not ensure the molecular connection between the oxidase and channel proteins. Homogenous distribution of the two molecules can also yield such a correlation if the ratio of expression does not vary too much among patches. However, it was suggested that at least two oxidase complexes have to cooperate in close contact for high-capacity e^- transport (Vignais, 2002), and NADPH–oxidase complexes tend to distribute in aggregates rather than evenly in phagocytes (Nugent et al., 1989; Wientjes et al., 1997). To account for the correlation between the two currents in excised patches, H^+ channels must therefore follow a similar distribution pattern.

In the second series of experiments we revisited the evidence indicating that the oxidase blocker DPI does not significantly affect H^+ currents. DPI failed to influence the activation kinetic and the amplitude of outward H^+ current in whole-cell perforated patch studies, and only reverted the slowing of the tail current induced by PMA (DeCoursey et al., 2000, 2001). The effect of DPI on the inward H^+ current was not reported in these studies, and no convincing explanation could be provided for the DPI effect on tail currents. Because tail currents through proton channels denote inward H^+ transport, we tested whether DPI affects the amplitude of steady-state inward proton currents in PMA-pretreated eosinophils. The inside-out patch approach allowed us to analyze systematically the effect of DPI and of NADPH by comparing the H^+ current amplitudes in the presence and complete absence of these compounds. Such a protocol could not be applied using the whole-cell technique, and allowed us to separate the direct effects of DPI on H^+ currents from its indirect effects caused by the inhibition of oxidase function.

These experiments indicate that only the inward, but not the outward H^+ transport is significantly affected by the simultaneous presence of DPI and NADPH on the cytosolic side of the patch membrane (Fig. 8). These observations are consistent with whole-cell results showing that DPI inhibits inward tail currents, but not outward proton transport through the H^+ channel. However, the interpretation becomes different, as under our conditions the local pH, [$O_2^{\cdot -}$] and electrical field changes generated by the oxidase are essentially absent when DPI is added before activation of the oxidase by NADPH. Therefore, the inhibition of inward H^+ flux observed under these conditions reflects the binding of NADPH and/or DPI. The requirement for reducing conditions for DPI to block the oxidase was observed in a cell-free system (Doussiere and Vignais, 1992) and may explain why a consistent DPI effect can only be observed in the presence of NADPH. A strong inhibition of inward H^+ current by DPI could be occasionally observed in the nominal absence of NADPH (Fig. S4), although the average effect was not significant. Together, these data indicate that DPI exerts either an unidirectional or a voltage-dependent block on the PMA-activated state of the proton channel. DPI appears to bind preferentially to the outer heme component of the oxidase (Doussiere et al., 1999), which becomes released by a coordinating histidine during oxidase activation (Doussiere et al., 1996). We suggested earlier that this histidine residue mediates inward H^+ flux, as the histidine reagent diethyl pirocarbonate blocked inward H^+ current activation and speeded up the tail current kinetic. Unlike DPI, however, diethyl pirocarbonate also reduced the amplitude and the activation kinetic of the outward current, suggesting that it reverted the shift in H^+ channel voltage dependence induced by oxidase activation. Although we cannot formally rule out the possibility that DPI and/or NADPH also shift back the H^+ channel activation threshold to more positive potentials, this possibility appears unlikely as DPI appears to specifically alter inward H^+ transport, both in whole-cell and excised patches. Our observations that agents known to bind to $gp91^{phox}$ and to alter the oxidase function also alter proton transport in excised patches containing a functional oxidase further suggest that the proton channel and the oxidase complex in normal phagocyte are closely connected.

In summary, human eosinophils express mainly one type of voltage-dependent proton channel whose function is linked to the NADPH–oxidase. Further experiments are required to ultimately prove whether or not the proton channel is contained within the NADPH–

oxidase complex, but the linear correlation between e^- and H^+ current amplitude, their similar rundown kinetics, and the effect of oxidase specific agents on H^+ currents suggests that the proton channel is either part of the oxidase complex or linked by a membrane-limited component. The ability to reliably measure electron currents in inside-out patches from human eosinophils allows us to directly address yet unresolved issues on the regulation of the phagocytic NADPH–oxidase. The inside-out patch technique may be particularly advantageous to study the highly regulated, but as yet mysterious processes involved in the down-regulation and inactivation of the oxidase.

We thank Elzbieta Huggler for her expert help in eosinophils preparation.

This work was supported by grant number 31-068317.02 from the Swiss National Science Foundation and by the National Science Foundation of Hungary (OTKA, TS 040865).

Olaf S. Andersen served as editor.

Submitted: 25 June 2003
Accepted: 13 October 2003

REFERENCES

Babior, B.M., J.D. Lambeth, and W. Nauseef. 2002. The neutrophil NADPH oxidase. *Arch. Biochem. Biophys.* 397:342–344.

Banfi, B., A. Maturana, S. Jaconi, S. Arnaudeau, T. Laforge, B. Sinha, E. Ligeti, N. Demaurex, and K.H. Krause. 2000. A mammalian H^+ channel generated through alternative splicing of the NADPH oxidase homolog NOH-1. *Science.* 287:138–142.

Banfi, B., G. Molnar, A. Maturana, K. Steger, B. Hegedus, N. Demaurex, and K.H. Krause. 2001. A Ca^{2+}-activated NADPH oxidase in testis, spleen, and lymph nodes. *J. Biol. Chem.* 276:37594–37601.

Banfi, B., J. Schrenzel, O. Nusse, D.P. Lew, E. Ligeti, K.H. Krause, and N. Demaurex. 1999. A novel H^+ conductance in eosinophils: unique characteristics and absence in chronic granulomatous disease. *J. Exp. Med.* 190:183–194.

Biberstine-Kinkade, K.J., F.R. DeLeo, R.I. Epstein, B.A. LeRoy, W.M. Nauseef, and M.C. Dinauer. 2001. Heme-ligating histidines in flavocytochrome b(558): identification of specific histidines in gp91(phox). *J. Biol. Chem.* 276:31105–31112.

Bokoch, G.M., and B.A. Diebold. 2002. Current molecular models for NADPH oxidase regulation by Rac GTPase. *Blood.* 100:2692–2696.

Briggs, R.T., D.B. Drath, M.L. Karnovsky, and M.J. Karnovsky. 1975. Localization of NADH oxidase on the surface of human polymorphonuclear leukocytes by a new cytochemical method. *J. Cell Biol.* 67:566–586.

Brown, G.E., M.Q. Stewart, H. Liu, V.L. Ha, and M.B. Yaffe. 2003. A novel assay system implicates $PtdIns_{3,4}P_2$, $PtdIns_3P$, and PKC δ in intracellular production of reactive oxygen species by the NADPH oxidase. *Mol. Cell.* 11:35–47.

Bukauskas, F.F., K. Jordan, A. Bukauskiene, M.V. Bennett, P.D. Lampe, D.W. Laird, and V.K. Verselis. 2000. Clustering of connexin 43-enhanced green fluorescent protein gap junction channels and functional coupling in living cells. *Proc. Natl. Acad. Sci. USA.* 97:2556–2561.

Cherny, V.V., and T.E. DeCoursey. 1999. pH-dependent inhibition of voltage-gated H^+ currents in rat alveolar epithelial cells by Zn^{2+} and other divalent cations. *J. Gen. Physiol.* 114:819–838.

Cherny, V.V., L.M. Henderson, W. Xu, L.L. Thomas, and T.E. DeCoursey. 2001. Activation of NADPH oxidase-related proton and electron currents in human eosinophils by arachidonic acid. *J. Physiol.* 535:783–794.

Cherny, V.V., R. Murphy, V. Sokolov, R.A. Levis, and T.E. DeCoursey. 2003. Properties of single voltage-gated proton channels in human eosinophils estimated by noise analysis and by direct measurement. *J. Gen. Physiol.* 121:615–628.

DeCoursey, T.E. 2003. Voltage-gated proton channels and other proton transfer pathways. *Physiol. Rev.* 83:475–579.

DeCoursey, T.E., and V.V. Cherny. 1993. Potential, pH, and arachidonate gate hydrogen ion currents in human neutrophils. *Biophys. J.* 65:1590–1598.

DeCoursey, T.E., V.V. Cherny, A.G. DeCoursey, W. Xu, and L.L. Thomas. 2001. Interactions between NADPH oxidase-related proton and electron currents in human eosinophils. *J. Physiol.* 535:767–781.

DeCoursey, T.E., V.V. Cherny, W. Zhou, and L.L. Thomas. 2000. Simultaneous activation of NADPH oxidase-related proton and electron currents in human neutrophils. *Proc. Natl. Acad. Sci. USA.* 97:6885–6889.

DeCoursey, T.E., D. Morgan, and V.V. Cherny. 2002. The gp91 (phox) component of NADPH oxidase is not a voltage-gated proton channel. *J. Gen. Physiol.* 120:773–779.

DeCoursey, T.E., D. Morgan, and V.V. Cherny. 2003. The voltage dependence of NADPH oxidase reveals why phagocytes need proton channels. *Nature.* 422:531–534.

DeLeo, F.R., J.B. Burritt, L. Yu, A.J. Jesaitis, M.C. Dinauer, and W.M. Nauseef. 2000. Processing and maturation of flavocytochrome b558 include incorporation of heme as a prerequisite for heterodimer assembly. *J. Biol. Chem.* 275:13986–13993.

Demaurex, N., S. Grinstein, M. Jaconi, W. Schlegel, D.P. Lew, and K.H. Krause. 1993. Proton currents in human granulocytes: regulation by membrane potential and intracellular pH. *J. Physiol.* 466:329–344.

Doussiere, J., J. Gaillard, and P.V. Vignais. 1996. Electron transfer across the O2-generating flavocytochrome b of neutrophils. Evidence for a transition from a low-spin state to a high-spin state of the heme iron component. *Biochemistry.* 35:13400–13410.

Doussiere, J., J. Gaillard, and P.V. Vignais. 1999. The heme component of the neutrophil NADPH oxidase complex is a target for aryliodonium compounds. *Biochemistry.* 38:3694–3703.

Doussiere, J., and P.V. Vignais. 1992. Diphenylene iodonium as an inhibitor of the NADPH oxidase complex of bovine neutrophils. Factors controlling the inhibitory potency of diphenylene iodonium in a cell-free system of oxidase activation. *Eur. J. Biochem.* 208:61–71.

Foubert, T.R., J.B. Burritt, R.M. Taylor, and A.J. Jesaitis. 2002. Structural changes are induced in human neutrophil cytochrome b by NADPH oxidase activators, LDS, SDS, and arachidonate: intermolecular resonance energy transfer between trisulfopyrenyl-wheat germ agglutinin and cytochrome b(558). *Biochim. Biophys. Acta.* 1567:221–231.

Geiszt, M., A. Kapus, and E. Ligeti. 2001. Chronic granulomatous disease: more than the lack of superoxide? *J. Leukoc. Biol.* 69:191–196.

Geletyuk, V.I., and V.N. Kazachenko. 1989. Single potential-dependent K+ channels and their oligomers in molluscan glial cells. *Biochim. Biophys. Acta.* 981:343–350.

Goldblatt, D., and A.J. Thrasher. 2000. Chronic granulomatous disease. *Clin. Exp. Immunol.* 122:1–9.

Gordienko, D.V., M. Tare, S. Parveen, C.J. Fenech, C. Robinson, and T.B. Bolton. 1996. Voltage-activated proton current in eosinophils from human blood. *J. Physiol.* 496:299–316.

Henderson, L.M., G. Banting, and J.B. Chappell. 1995. The arachi-

donate-activable, NADPH oxidase-associated H+ channel. Evidence that gp91-phox functions as an essential part of the channel. *J. Biol. Chem.* 270:5909–5916.

Henderson, L.M., J.B. Chappell, and O.T. Jones. 1987. The superoxide-generating NADPH oxidase of human neutrophils is electrogenic and associated with an H+ channel. *Biochem. J.* 246:325–329.

Henderson, L.M., J.B. Chappell, and O.T. Jones. 1988. Internal pH changes associated with the activity of NADPH oxidase of human neutrophils. Further evidence for the presence of an H+ conducting channel. *Biochem. J.* 251:563–567.

Henderson, L.M., and R.W. Meech. 1999. Evidence that the product of the human X-linked CGD gene, gp91-phox, is a voltage-gated H^+ pathway. *J. Gen. Physiol.* 114:771–786.

Henderson, L.M., and R.W. Meech. 2002. Proton conduction through gp91(phox). *J. Gen. Physiol.* 120:759–765.

Hille, B. 1992. Ionic Channels in Excitable Membranes. 2nd ed. Sinauer Associates Inc., Sunderland, MA. 607 pp.

Hymel, L., J. Striessnig, H. Glossmann, and H. Schindler. 1988. Purified skeletal muscle 1, 4-dihydropyridine receptor forms phosphorylation-dependent oligomeric calcium channels in planar bilayers. *Proc. Natl. Acad. Sci. USA.* 85:4290–4294.

Kanai, F., H. Liu, S.J. Field, H. Akbary, T. Matsuo, G.E. Brown, L.C. Cantley, and M.B. Yaffe. 2001. The PX domains of p47phox and p40phox bind to lipid products of PI_3K. *Nat. Cell Biol.* 3:675–678.

Kapus, A., R. Romanek, and S. Grinstein. 1994. Arachidonic acid stimulates the plasma membrane H^+ conductance of macrophages. *J. Biol. Chem.* 269:4736–4745.

Kapus, A., R. Romanek, A.Y. Qu, O.D. Rotstein, and S. Grinstein. 1993. A pH-sensitive and voltage-dependent proton conductance in the plasma membrane of macrophages. *J. Gen. Physiol.* 102: 729–760.

Kapus, A., K. Szaszi, and E. Ligeti. 1992. Phorbol 12-myristate 13-acetate activates an electrogenic H^+-conducting pathway in the membrane of neutrophils. *Biochem. J.* 281:697–701.

Karathanassis, D., R.V. Stahelin, J. Bravo, O. Perisic, C.M. Pacold, W. Cho, and R.L. Williams. 2002. Binding of the PX domain of p47(phox) to phosphatidylinositol 3, 4-bisphosphate and phosphatidic acid is masked by an intramolecular interaction. *EMBO J.* 21:5057–5068.

Lapouge, K., S.J. Smith, Y. Groemping, and K. Rittinger. 2002. Architecture of the p40-p47-p67phox complex in the resting state of the NADPH oxidase. A central role for p67phox. *J. Biol. Chem.* 277:10121–10128.

Ligeti, E., J. Doussiere, and P.V. Vignais. 1988. Activation of the O2(.−)-generating oxidase in plasma membrane from bovine polymorphonuclear neutrophils by arachidonic acid, a cytosolic factor of protein nature, and nonhydrolyzable analogues of GTP. *Biochemistry.* 27:193–200.

Marx, S.O., K. Ondrias, and A.R. Marks. 1998. Coupled gating between individual skeletal muscle Ca^{2+} release channels (ryanodine receptors). *Science.* 281:818–821.

Maturana, A., S. Arnaudeau, S. Ryser, B. Banfi, J.P. Hossle, W. Schlegel, K.H. Krause, and N. Demaurex. 2001. Heme histidine ligands within gp91(phox) modulate proton conduction by the phagocyte NADPH oxidase. *J. Biol. Chem.* 276:30277–30284.

Maturana, A., K.H. Krause, and N. Demaurex. 2002. NOX family NADPH oxidases: do they have built-in proton channels? *J. Gen. Physiol.* 120:781–786.

Morgan, D., V.V. Cherny, M.O. Price, M.C. Dinauer, and T.E. DeCoursey. 2002. Absence of proton channels in COS-7 cells expressing functional NADPH oxidase components. *J. Gen. Physiol.* 119:571–580.

Moskwa, P., M.C. Dagher, M.H. Paclet, F. Morel, and E. Ligeti. 2002. Participation of Rac GTPase activating proteins in the deactivation of the phagocytic NADPH oxidase. *Biochemistry.* 41:10710–10716.

Nanda, A., J.T. Curnutte, and S. Grinstein. 1994. Activation of H+ conductance in neutrophils requires assembly of components of the respiratory burst oxidase but not its redox function. *J. Clin. Invest.* 93:1770–1775.

Nugent, J.H., W. Gratzer, and A.W. Segal. 1989. Identification of the haem-binding subunit of cytochrome b-245. *Biochem. J.* 264: 921–924.

Quinn, M.T., C.A. Parkos, L. Walker, S.H. Orkin, M.C. Dinauer, and A.J. Jesaitis. 1989. Association of a Ras-related protein with cytochrome b of human neutrophils. *Nature.* 342:198–200.

Schindler, H., F. Spillecke, and E. Neumann. 1984. Different channel properties of Torpedo acetylcholine receptor monomers and dimers reconstituted in planar membranes. *Proc. Natl. Acad. Sci. USA.* 81:6222–6226.

Schreibmayer, W., H.A. Tritthart, and H. Schindler. 1989. The cardiac sodium channel shows a regular substate pattern indicating synchronized activity of several ion pathways instead of one. *Biochim. Biophys. Acta.* 986:172–186.

Schrenzel, J., D.P. Lew, and K.H. Krause. 1996. Proton currents in human eosinophils. *Am. J. Physiol.* 271:C1861–C1871.

Schrenzel, J., L. Serrander, B. Banfi, O. Nusse, R. Fouyouzi, D.P. Lew, N. Demaurex, and K.H. Krause. 1998. Electron currents generated by the human phagocyte NADPH oxidase. *Nature.* 392: 734–737.

Shiose, A., and H. Sumimoto. 2000. Arachidonic acid and phosphorylation synergistically induce a conformational change of p47phox to activate the phagocyte NADPH oxidase. *J. Biol. Chem.* 275:13793–13801.

Stahelin, R.V., A. Burian, K.S. Bruzik, D. Murray, and W. Cho. 2003. Membrane binding mechanisms of the PX domains of NADPH oxidase p40phox and p47phox. *J. Biol. Chem.* 278:14469–14479.

Tanemoto, M., A. Fujita, K. Higashi, and Y. Kurachi. 2002. PSD-95 mediates formation of a functional homomeric Kir5. 1 channel in the brain. *Neuron.* 34:387–397.

Touret, N., and S. Grinstein. 2002. Voltage-gated proton "channels": a spectator's viewpoint. *J. Gen. Physiol.* 120:767–771.

Vignais, P.V. 2002. The superoxide-generating NADPH oxidase: structural aspects and activation mechanism. *Cell. Mol. Life Sci.* 59:1428–1459.

Wallach, T.M., and A.W. Segal. 1996. Stoichiometry of the subunits of flavocytochrome b558 of the NADPH oxidase of phagocytes. *Biochem. J.* 320:33–38.

Wang, S., H. Yue, R.B. Derin, W.B. Guggino, and M. Li. 2000. Accessory protein facilitated CFTR-CFTR interaction, a molecular mechanism to potentiate the chloride channel activity. *Cell.* 103: 169–179.

Wientjes, F.B., A.W. Segal, and J.H. Hartwig. 1997. Immunoelectron microscopy shows a clustered distribution of NADPH oxidase components in the human neutrophil plasma membrane. *J. Leukoc. Biol.* 61:303–312.